

Sphingosine 1-phosphate regulates regeneration and fibrosis after liver injury via sphingosine 1-phosphate receptor 2

Hitoshi Ikeda,^{1,*†} Naoko Watanabe,^{*,†} Isao Ishii,[§] Tatsuo Shimosawa,^{*} Yukio Kume,^{*} Tomoaki Tomiya,[†] Yukiko Inoue,[†] Takako Nishikawa,[†] Natsuko Ohtomo,[†] Yasushi Tanoue,[†] Satoko Iitsuka,^{*} Ryoto Fujita,^{*} Masao Omata,[†] Jerold Chun,^{**} and Yutaka Yatomi^{*}

Department of Clinical Laboratory Medicine,^{*} and Department of Gastroenterology,[†] Graduate School of Medicine, The University of Tokyo, 7-3-1 Hongo, Bunkyo-ku, Tokyo, Japan; Department of Molecular and Cellular Neurobiology,[§] Gunma University Graduate School of Medicine, Gunma, Japan; and Department of Molecular Biology,^{**} Helen L. Dorris Child and Adolescent Neuropsychiatric Disorder Institute, The Scripps Research Institute, La Jolla, CA

Abstract Sphingosine 1-phosphate (S1P), a bioactive lipid mediator, stimulates proliferation and contractility in hepatic stellate cells, the principal matrix-producing cells in the liver, and inhibits proliferation via S1P receptor 2 (S1P₂) in hepatocytes in rats in vitro. A potential role of S1P and S1P₂ in liver regeneration and fibrosis was examined in S1P₂-deficient mice. Nuclear 5-bromo-2'-deoxy-uridine labeling, proliferating cell nuclear antigen (PCNA) staining in hepatocytes, and the ratio of liver weight to body weight were enhanced at 48 h in S1P₂-deficient mice after a single carbon tetrachloride (CCl₄) injection. After dimethylnitrosamine (DMN) administration with a lethal dose, PCNA staining in hepatocytes was enhanced at 48 h and survival rate was higher in S1P₂-deficient mice. Serum aminotransferase level was unaltered in those mice compared with wild-type mice in both CCl₄- and DMN-induced liver injury, suggesting that S1P₂ inactivation accelerated regeneration not as a response to enhanced liver damage. After chronic CCl₄ administration, fibrosis was less apparent, with reduced expression of smooth-muscle α -actin-positive cells in the livers of S1P₂-deficient mice, suggesting that S1P₂ inactivation ameliorated CCl₄-induced fibrosis due to the decreased accumulation of hepatic stellate cells. **■** Thus, S1P plays a significant role in regeneration and fibrosis after liver injury via S1P₂.—Ikeda, H., N. Watanabe, I. Ishii, T. Shimosawa, Y. Kume, T. Tomiya, Y. Inoue, T. Nishikawa, N. Ohtomo, Y. Tanoue, S. Iitsuka, R. Fujita, M. Omata, J. Chun, and Y. Yatomi. **Sphingosine 1-phosphate regulates regeneration and fibrosis after liver injury via sphingosine 1-phosphate receptor 2.** *J. Lipid Res.* 2009. 50: 556–564.

Supplementary key words liver regeneration • liver fibrosis • hepatocyte • hepatic stellate cell • hepatic myofibroblast

This work was supported by the Japanese Society of Laboratory Medicine Fund for the Promotion of Scientific Research (H.I.) and by National Institutes of Health Grants NS-048478 and R01 DA-019674 (J.C.).

Manuscript received 23 September 2008 and in revised form 24 October 2008.

Published, JLR Papers in Press, October 27, 2008.

DOI 10.1194/jlr.M800496-JLR200

Sphingosine 1-phosphate (S1P), which elicits a wide variety of cell responses (1), has emerged as a novel lipid intracellular mediator. S1P was shown to act as an intracellular second messenger of platelet-derived growth factor and serum in their mitogenic actions in cultured fibroblasts (2, 3), and furthermore, intracellular levels of S1P and ceramide were reported to determine cell survival or death (4, 5). However, evidence indicating that S1P also acts as an extracellular mediator has been reported; some of the diverse effects of S1P, such as stimulation of cell proliferation or contractility, are known to be sensitive to pertussis toxin (6) or ADP-ribosyltransferase C3 from *Clostridium botulinum* (7, 8), suggesting that S1P may activate a receptor coupled to G protein(s). Indeed, recent investigation has revealed that S1P acts through at least five high-affinity G protein-coupled receptors referred to as S1P_{1–5} (9, 10). Regarding the source of S1P in vivo, it is shown to be stored in platelets (11), and recent data using conditional knockouts of sphingosine kinases support release of S1P from erythrocytes (12, 13). These findings suggest that S1P has normal in vivo roles as well as potentially pathophysiological roles as a circulating paracrine mediator, a view further supported by the phenotypes of S1P receptor mutants (10, 14, 15).

S1P receptors are also expressed in the liver (14). To investigate the function of S1P in liver pathophysiology, we have determined the effect of S1P on liver cells in culture. We first demonstrated that S1P stimulates proliferation and contractility in rat hepatic stellate cells in culture; the stimulation of proliferation is pertussis toxin-sensitive,

Abbreviations: ALT, alanine aminotransferase; ALP, alkaline phosphatase; BrdU, 5-bromo-2'-deoxy-uridine; CCl₄, carbon tetrachloride; DMN, dimethylnitrosamine; PCNA, proliferating cell nuclear antigen; S1P, sphingosine 1-phosphate.

¹ To whom correspondence should be addressed.

e-mail: ikeda-lim@h.u-tokyo.ac.jp

and the stimulation of contractility is C3 exotoxin-sensitive (16). This stimulatory effect of SIP on contractility in those cells was found to be via SIP_2 with Rho activation (17). On the other hand, we revealed that SIP inhibits proliferation in cultured rat hepatocytes. With the use of a specific antagonist to SIP_2 and C3 exotoxin, this inhibitory effect of SIP on hepatocyte proliferation in culture involved Rho activation via SIP_2 (18). Furthermore, the administration of SIP in 70% hepatectomized rats indeed reduces a response of hepatocytes to synthesize DNA (18).

Irrespective of the insults, such as viruses, alcohol abuse, or drugs, the regenerative and wound-healing responses generally occur in the liver after the injury, and the persistence of these responses may result in liver fibrosis (19, 20). Hepatocytes play a major role in liver regeneration (19) as do hepatic stellate cells in the wound-healing response, and hence, liver fibrosis (20). The enhanced proliferation and contractility of hepatic stellate cells are among the main features of liver fibrosis (21, 22). Although our previous evidence was obtained mainly by *in vitro* studies and indicated a pharmacologically inhibitory effect of SIP

on liver regeneration *in vivo*, it raised the possibility that SIP, and potentially SIP_2 , might play a pathophysiological role in the liver after the injury. Thus, we planned to extend our study using SIP_2 -deficient mice to clarify this point.

In this context, Serrier-Lanneau et al. (23) recently reported that the wound-healing response to acute liver injury elicited by carbon tetrachloride (CCl_4) was reduced in $SIP_2^{-/-}$ mice with reduced accumulation of hepatic myofibroblasts and that hepatic myofibroblasts isolated from $SIP_2^{-/-}$ mice did not proliferate in response to SIP. There is controversy as to whether hepatic myofibroblasts are distinct from hepatic stellate cells. Hepatic myofibroblasts have been studied as the cells developed from hepatic stellate cells by transdifferentiation (24–27). In contrast, hepatic myofibroblasts have been reported to belong to a cell population different from hepatic stellate cells (28). Whatever the case, hepatic myofibroblasts have been assumed to be a principle matrix-producing cell of the diseased liver (29). On the other hand, the regenerative response after a single injection of CCl_4 in $SIP_2^{-/-}$ mice was not different from that in wild-type mice, suggesting that SIP_2 inac-

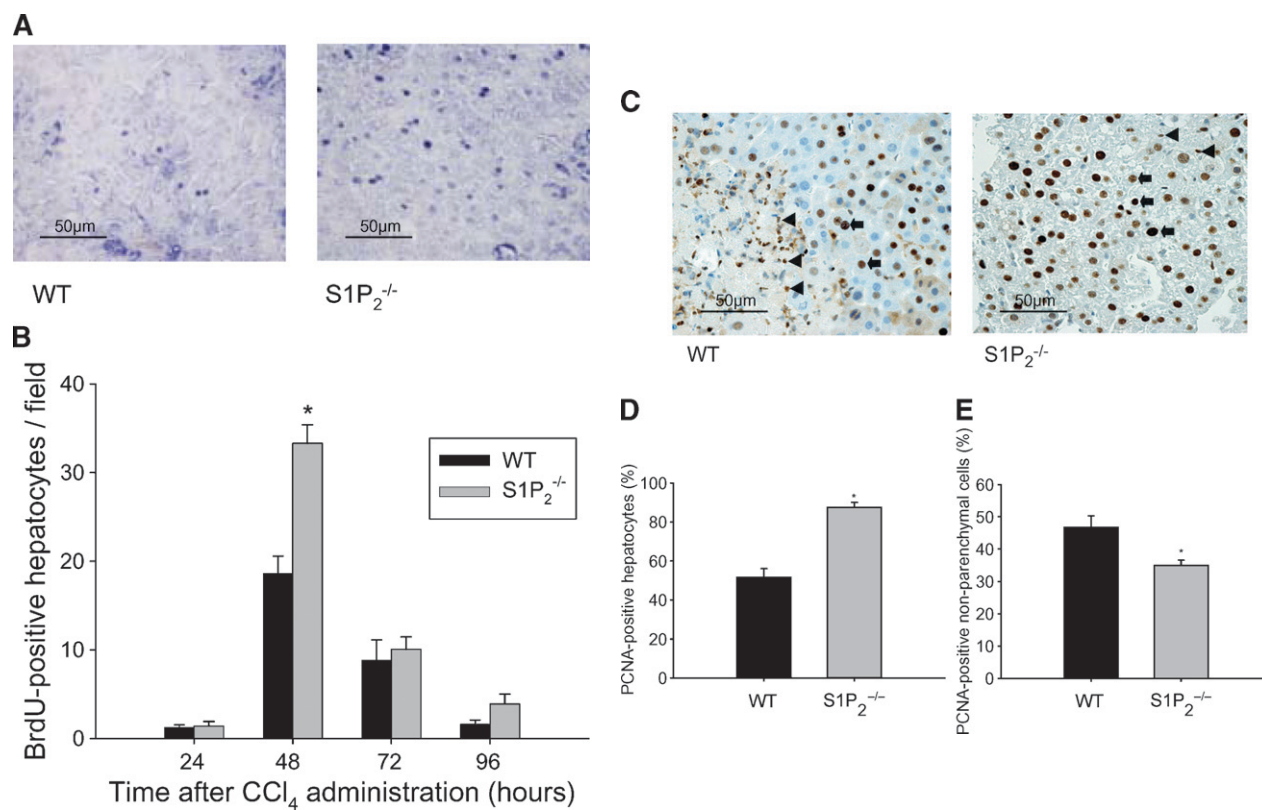


Fig. 1. Regenerative response in hepatocytes and nonparenchymal cells of wild-type and $SIP_2^{-/-}$ livers in acute injury induced by carbon tetrachloride (CCl_4). A single injection of CCl_4 was performed in wild-type (WT) and $SIP_2^{-/-}$ mice. 5-Bromo-2'-deoxy-uridine (BrdU) was injected intraperitoneally at 1 h before euthanization at 24, 48, 72, and 96 h after CCl_4 injection. The nuclear labeling in hepatocytes was determined using a BrdU labeling and detection kit II. Representative BrdU labeling in the livers of wild-type and $SIP_2^{-/-}$ mice at 48 h after CCl_4 injection is shown (A). Bar = 50 μ m. The number of BrdU-positive cells was determined as the mean of five random areas at 400-fold magnification in each section (B). Columns and bars represent means \pm SEM of four animals. Immunohistochemical analysis of proliferating cell nuclear antigen (PCNA) was also done using a PCNA staining kit. Representative photomicrographs of the liver of wild-type and $SIP_2^{-/-}$ mice at 48 h after CCl_4 injection are shown (C). Bar = 50 μ m. Arrows indicate positive hepatocytes, and arrowheads, positive nonparenchymal cells. The percentages of PCNA-positive hepatocytes (D) and nonparenchymal cells (E) were determined with five random areas at 400-fold magnification in each section. Columns and bars represent means \pm SEM of four animals. The asterisk indicates a significant difference from wild type in Student's *t*-test ($P < 0.05$).

tivation did not affect hepatocyte regeneration (23). With these findings, we aimed to perform more-detailed examination of hepatocyte regeneration in acute liver injury elicited by dimethylnitrosamine (DMN) in addition to CCl_4 and to determine whether reduced wound-healing response could lead to reduced liver fibrosis after chronic CCl_4 administration in $\text{SIP}_2^{-/-}$ mice.

MATERIALS AND METHODS

Animals

Heterozygous $\text{SIP}_2^{+/-}$ mice were originally generated by our group on the (129/Sv \times 129/J) F_1 (an embryonic stem cell origin)/C57BL/6N (a blastocyst origin) mixed background (30). In this study, they were backcrossed onto the inbred C57BL/6N strain (Clea Japan, Tokyo, Japan) for 7–8 generations to achieve >99.2% genetic homogeneity, and the obtained $\text{SIP}_2^{+/-}$ mice

were bred to produce $\text{SIP}_2^{-/-}$ mice. Deletion of SIP_2 in these $\text{SIP}_2^{-/-}$ mice has been repeatedly confirmed by the complete absence of *sIIP2* gene expression in tissues (e.g., adult lung, spleen, brain, heart, cochlea, and embryonic fibroblasts) in which *sIIP2* is normally expressed (15, 30, 31) as well as the specific appearance or disappearance of some SIP-mediated cellular signaling/systemic effects (15, 30–32). Age-matched wild-type C57BL/6N mice were used as controls. They were fed a standard pelleted diet and water ad libitum under normal laboratory conditions of 12 h light/dark cycles. All animals received humane care, and the research was conducted in conformity with Public Health Service policy on the humane care and use of laboratory animals. The experimental protocol was approved by the Animal Research Committee of the University of Tokyo and followed National Institutes of Health guidelines for the care and use of laboratory animals.

CCl_4 treatment

To assess the responses to a single CCl_4 administration, male and female wild-type and $\text{SIP}_2^{-/-}$ mice, 8–10 weeks of age, were

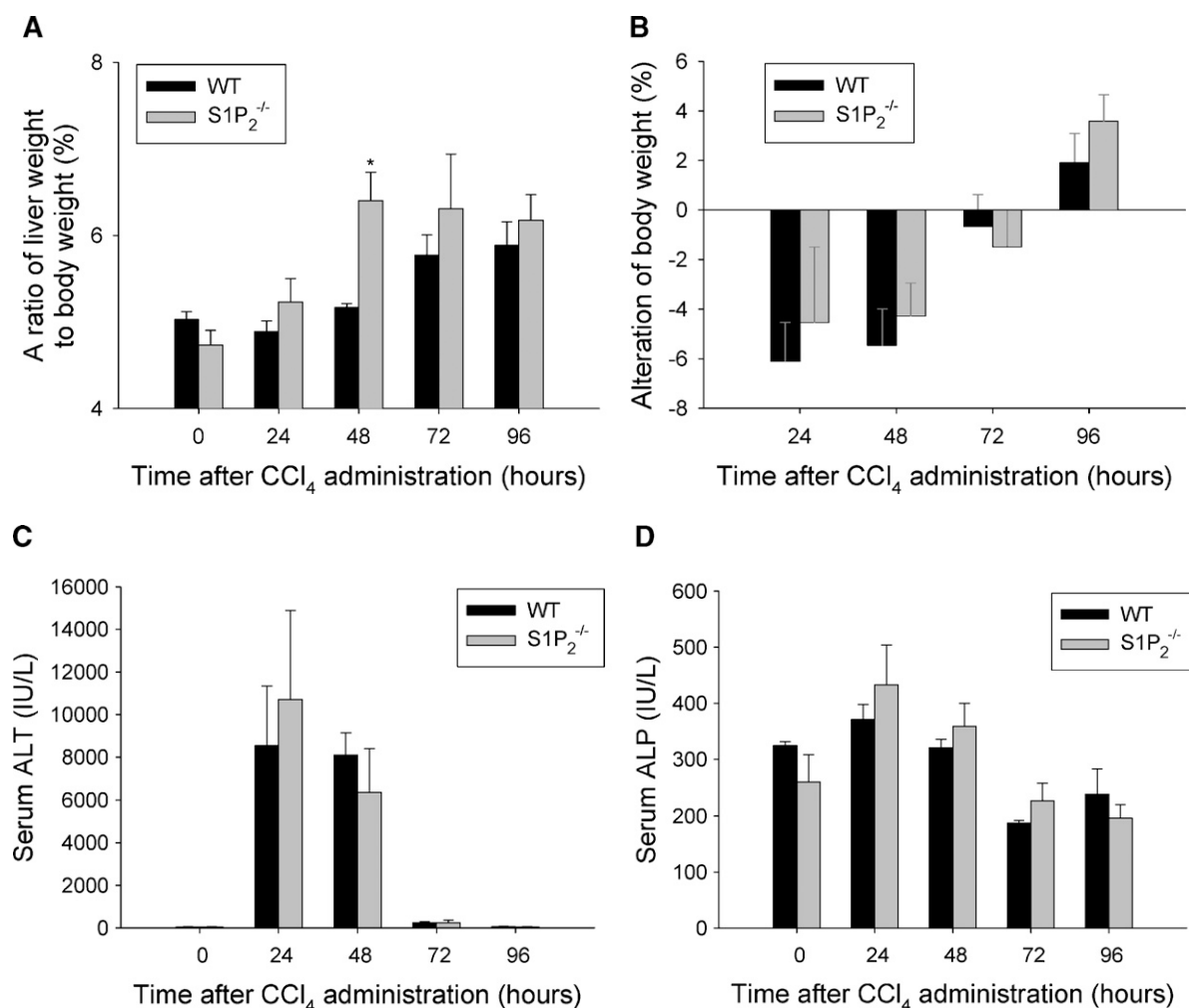


Fig. 2. The ratio of liver weight to body weight, body weight loss, and liver function tests in wild-type and $\text{SIP}_2^{-/-}$ mice in acute liver injury induced by CCl_4 . A single injection of CCl_4 was performed in wild-type (WT) and $\text{SIP}_2^{-/-}$ mice. The ratio of liver weight to body weight was measured in untreated wild-type and $\text{SIP}_2^{-/-}$ mice from 24 to 96 h at euthanization after CCl_4 injection (A). The alteration of body weight was determined by comparison of body weights before CCl_4 injection with those at 24, 48, 72, and 96 h after CCl_4 injection (B). Serum concentrations of alanine aminotransferase (ALT) (C) and alkaline phosphatase (ALP) (D) were measured in wild-type and $\text{SIP}_2^{-/-}$ mice at 24, 48, 72, and 96 h after CCl_4 injection. Columns and bars represent means \pm SEM of four animals. The asterisk indicates a significant difference from wild type in Student's *t*-test ($P < 0.05$).

injected intraperitoneally with 0.5 ml/kg body weight of CCl₄ dissolved in the same amount of olive oil (1:1) (23), in which liver injury, assessed by serum aminotransferase level, was nongender specific. To develop liver fibrosis, female wild-type and S1P₂^{-/-} mice, 8 weeks of age, were injected intraperitoneally with 1 ml/kg body weight of CCl₄ dissolved in the same amount of olive oil (1:1), twice a week for 4 weeks (33, 34). Control mice received injection of the carrier (olive oil) alone. Each group consisted of four to five mice. For the experiment on chronic CCl₄ treatment, the livers were harvested at 4 days after the end of the administration.

DMN treatment

Male and female wild-type and S1P₂^{-/-} mice, 8–10 weeks of age, were injected intraperitoneally with 15 mg/kg body weight DMN dissolved in HBSS (0.3%) (GIBCO) (35), in which liver injury, assessed by serum aminotransferase level, was nongender specific.

Measurement of nuclear labeling by 5-bromo-2'-deoxy-uridine

One hour before euthanization, 50 mg/4 ml/kg body weight of 5-bromo-2'-deoxy-uridine (BrdU) (Roche Molecular Biochemicals, Mannheim, Germany) was injected intraperitoneally, and then the mice were euthanized at 24, 48, 72, and 96 h after CCl₄ administration. The liver was excised, immediately fixed in 10% formalin, and embedded in paraffin. The nuclear labeling was measured using BrdU labeling and detection kit II (Roche Molecular Biochemicals). The number of BrdU-positive hepatocytes was determined as the mean of five random areas at 400-fold magnification in each section.

Immunohistochemical analysis of proliferating cell nuclear antigen

Immunohistochemical staining for proliferating cell nuclear antigen (PCNA) was performed in liver tissue using a PCNA staining kit (Zymed Laboratories) in accordance with the protocol specified by the manufacturer. The ratio of PCNA-positive hepatocytes to all hepatocytes was determined with five random areas at 400-fold magnification in each section in CCl₄-treated mice and with ten random areas in DMN-treated mice, because submassive hemorrhagic necrosis was focally found in DMN-treated livers as previously described (36). The percentage of PCNA-positive nonparenchymal cells was determined with five random areas at 400-fold magnification in each section in CCl₄-treated mice.

Measurement of liver function

The serum levels of alanine aminotransferase (ALT) and alkaline phosphatase (ALP) were determined using an automated analyzer (Hitachi 7170; Hitachi Instruments Service Co., Ltd., Tokyo, Japan).

Histological analysis of fibrosis

Tissue sections (4 μm thick) of liver specimens fixed in formalin and embedded in paraffin were analyzed with Masson's trichrome staining (37). The microscopic fields (five per each slide) were blindly selected and captured with the aid of the Nikon Digital Camera DXM1200 (NIKON, Japan). A fibrous portion stained in blue was extracted, and the extent of liver fibrosis was quantified by the technique reported previously (38) by calculating the area of fibrosis/area of section using image analysis software of the public domain Scion Image (Scion Corporation).

Immunohistochemical analysis of smooth-muscle α-actin

Immunohistochemical analysis of smooth-muscle α-actin was performed in liver tissue fixed in formalin and embedded in par-

affin using a Vector M.O.M. immunodetection kit (Vector Laboratories, Burlingame, CA) in accordance with the protocol specified by the manufacturer, with a 1:5 dilution of mouse monoclonal antibody to smooth-muscle α-actin (Sigma). The quantitation of the positive staining area for smooth-muscle α-actin was performed blindly on four or five liver fragments per animal using the computer software of the public domain Scion Image developed by the Scion Corporation.

Statistical analysis

Data are represented as mean ± SEM. An ANOVA followed by Tukey's honest significance differences test (Tukey's HSD) or Student's *t*-test were used to determine whether significant differences existed between groups. Fisher's exact test was performed when appropriate. Differences were considered to be significant at *P* values of <0.05.

RESULTS

Regenerative response of hepatocytes to CCl₄-induced acute liver injury was enhanced in S1P₂^{-/-} mice

After a single CCl₄ administration, DNA synthesis of hepatocytes determined by BrdU labeling peaked at 48 h in

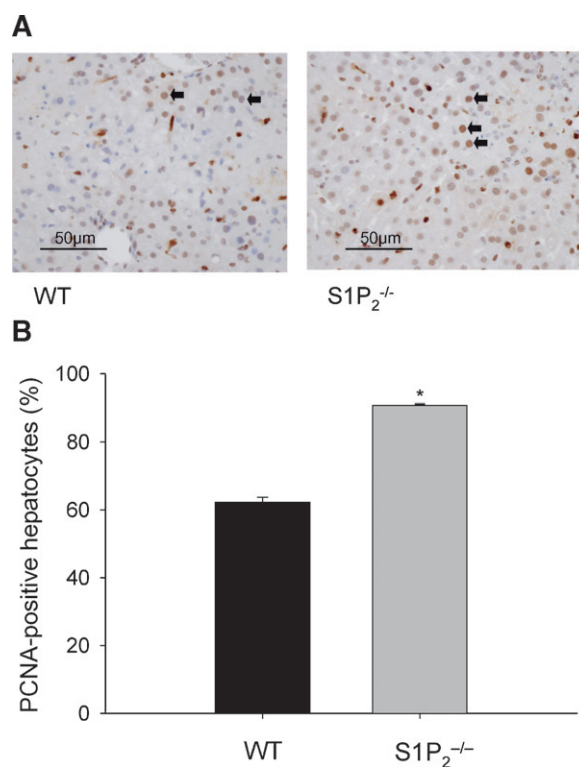


Fig. 3. PCNA-positive hepatocytes of wild-type and S1P₂^{-/-} livers in acute liver injury induced by dimethylnitrosamine (DMN). A single injection of DMN was performed in wild-type (WT) and S1P₂^{-/-} mice. Immunohistochemical analysis of PCNA was done using a PCNA staining kit. Representative photomicrographs of the liver of wild-type and S1P₂^{-/-} mice at 48 h after DMN injection are shown (A). Bar = 50 μm. Arrows indicate positive hepatocytes. The percentage of PCNA-positive hepatocytes was determined with ten random areas at 400-fold magnification in each section (B). Columns and bars represent means ± SEM of four animals. The asterisk indicates a significant difference from wild type in Student's *t*-test (*P* < 0.05).

both wild-type and $S1P_2^{-/-}$ mice (Fig. 1). As depicted in Fig. 1, BrdU-positive hepatocytes seemed more apparent in $S1P_2^{-/-}$ mice than in wild-type mice (Fig. 1A) at 48 h after CCl_4 administration, and in fact, the number of BrdU-positive hepatocytes at 48 h after CCl_4 administration in $S1P_2^{-/-}$ mice was significantly increased by 1.8-fold compared with wild-type mice (Fig. 1B). On the other hand, BrdU-positive hepatocytes were not found in both wild-type

and $S1P_2^{-/-}$ mice treated with olive oil alone. We next performed immunohistochemical analysis of PCNA in wild-type and $S1P_2^{-/-}$ livers after a single CCl_4 administration. As demonstrated in Fig. 1, PCNA-positive hepatocytes were more apparent in $S1P_2^{-/-}$ mice than in wild-type mice (Fig. 1C) at 48 h after CCl_4 administration. The number of PCNA-positive hepatocytes significantly increased by 1.7-fold in $S1P_2^{-/-}$ mice compared with wild-type mice (Fig. 1D).

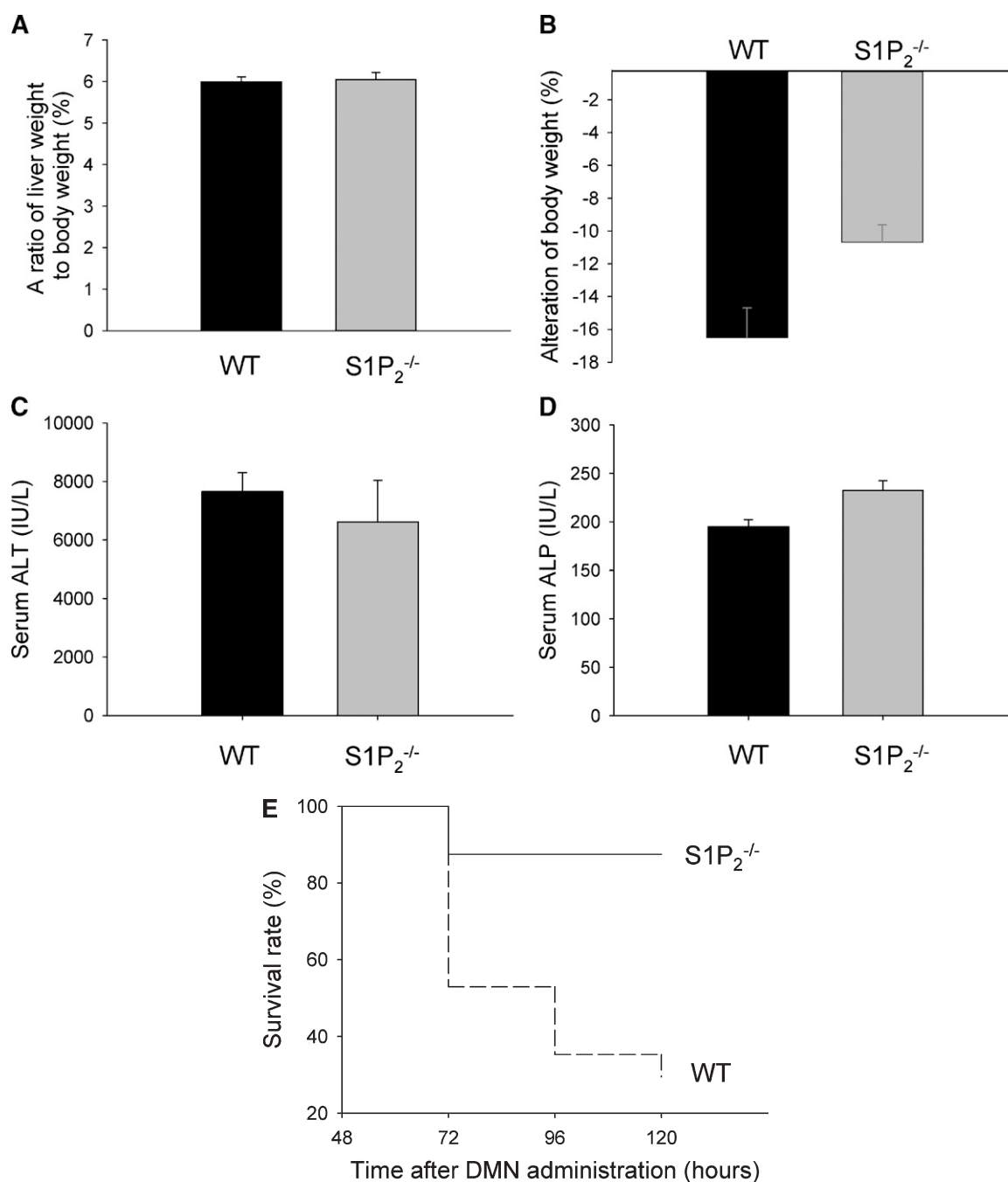


Fig. 4. The ratio of liver weight to body weight, body weight loss, liver function test, and survival rate in wild-type and $S1P_2^{-/-}$ mice in acute liver injury induced by DMN. A single injection of DMN was performed in wild-type (WT) and $S1P_2^{-/-}$ mice. The ratio of liver weight to body weight (A), body weight loss (B), and serum concentration of ALT (C) and ALP (D) were measured at 48 h after DMN injection. Columns and bars represent means \pm SEM of four animals. Survival rate was also determined in wild-type ($n = 17$) and $S1P_2^{-/-}$ ($n = 16$) mice up to 120 h after DMN injection (E). Significantly higher survival rate in $S1P_2^{-/-}$ mice was determined at 96 and 120 h after DMN injection in Fisher's exact test ($P < 0.05$).

On the other hand, it is of note that PCNA-positive non-parenchymal cells were less apparent in $SIP_2^{-/-}$ mice compared with wild-type mice (Fig. 1C). The percentage of PCNA-positive nonparenchymal cells in $SIP_2^{-/-}$ mice was reduced to 62% of that in wild-type mice (Fig. 1E). In both wild-type and $SIP_2^{-/-}$ mice treated with olive oil alone, PCNA-positive cells were not determined. These results suggest that the regenerative response after CCl_4 administration is enhanced in hepatocytes, but reduced in nonparenchymal cells in $SIP_2^{-/-}$ mice.

We then analyzed both liver weight and body weight at euthanization after a single injection of CCl_4 . The ratio of liver weight to body weight was significantly higher in $SIP_2^{-/-}$ mice than in wild-type mice at 48 h after CCl_4 administration, but not different between wild-type and $SIP_2^{-/-}$ mice at 24, 72, and 96 h (Fig. 2A). Both wild-type and $SIP_2^{-/-}$ mice lost their body weight maximally at 24 h after CCl_4 administration and then gradually gained weight up to 96 h, as shown in Fig. 2B. The alterations of body weight after CCl_4 administration were not different between wild-type and $SIP_2^{-/-}$ mice. These results suggest that the regenerative response in the liver after CCl_4 administration is enhanced in $SIP_2^{-/-}$ mice.

To examine the extent of liver damage elicited by CCl_4 administration, serum levels of ALT and ALP were measured up to 96 h after treatment. Serum ALT level peaked at 24 h after CCl_4 administration and was not significantly different between wild-type and $SIP_2^{-/-}$ mice (Fig. 2C), as previously reported (23). Furthermore, serum level of ALP was not different between wild-type and $SIP_2^{-/-}$ mice (Fig. 2D). These results suggest that the extent of liver damage caused by a single injection of CCl_4 was not different in $SIP_2^{-/-}$ mice compared with wild-type mice.

Enhanced regenerative response of hepatocytes to DMN-induced acute liver injury led to increased survival rate in $SIP_2^{-/-}$ mice

To determine whether the enhanced hepatocyte regeneration in $SIP_2^{-/-}$ mice could be the specific phenomenon in CCl_4 -induced acute liver injury, the regenerative response of hepatocytes in $SIP_2^{-/-}$ mice was also examined in DMN-induced acute liver injury (35). In this experiment, BrdU labeling was not suitable for determining the proliferative response, because significant amounts of ascites were found in both wild-type and $SIP_2^{-/-}$ mice in which BrdU was administered intraperitoneally. Thus, we determined the proliferative response by PCNA staining. At 48 h after DMN administration, PCNA-positive hepatocytes were more apparent in $SIP_2^{-/-}$ mice than in wild-type mice (Fig. 3A). The percentage of PCNA-positive hepatocytes increased by 1.5-fold in $SIP_2^{-/-}$ mice compared with wild-type mice (Fig. 3B). On the other hand, PCNA-positive hepatocytes were not found in both wild-type and $SIP_2^{-/-}$ mice treated with vehicle alone. This result suggests that the regenerative response is also enhanced after DMN administration in hepatocytes in $SIP_2^{-/-}$ mice. At the same time point, the ratio of liver weight to body weight was not different between wild-type and $SIP_2^{-/-}$ mice (Fig. 4A), and the trend of more body weight loss in wild-type mice was noted ($P =$

0.05116) (Fig. 4B). Serum levels of ALT (Fig. 4C) and ALP (Fig. 4D) were not different between wild-type and $SIP_2^{-/-}$ mice at the same time point, suggesting that the extent of DMN-induced liver damage was not different in $SIP_2^{-/-}$ mice compared with wild-type mice.

Although we next planned to determine the regenerative response in hepatocytes in wild-type and $SIP_2^{-/-}$ mice beyond 48 h after DMN administration, a substantial number of wild-type mice were found to be dead at 72 h after DMN administration. Thus, our experiment was changed to determine survival rate of wild-type and $SIP_2^{-/-}$ mice with DMN intoxication. As shown in Fig. 4E, survival rate was significantly higher in $SIP_2^{-/-}$ mice compared with wild-type mice at 96 to 120 h after DMN injection. Thus, increased regenerative response in hepatocytes after DMN intoxication may lead to increased survival rate in $SIP_2^{-/-}$ mice.

Liver fibrosis induced by chronic CCl_4 administration was reduced in $SIP_2^{-/-}$ mice

Next, the role of SIP_2 receptor signaling in liver fibrosis was examined in chronic liver injury elicited by CCl_4 . In wild-type mice, chronic administration of CCl_4 for 4 weeks caused an extensive accumulation of extracellular matrices

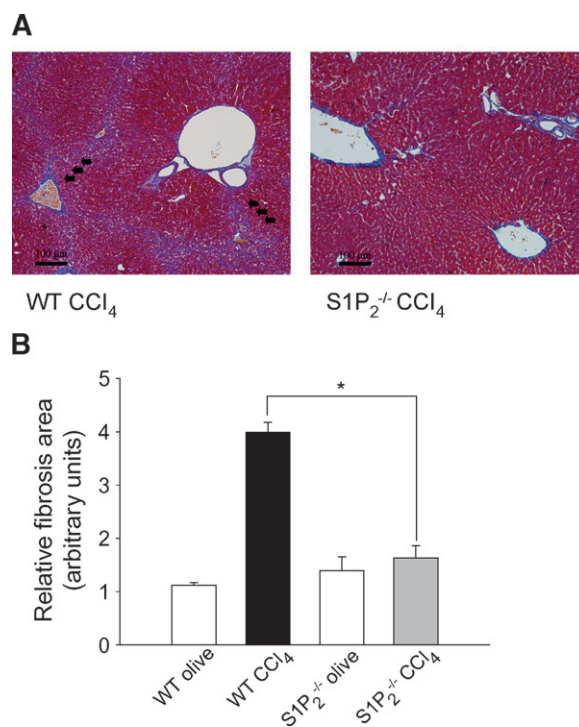


Fig. 5. Liver fibrosis in wild-type and $SIP_2^{-/-}$ mice after chronic CCl_4 administration. Wild-type (WT) and $SIP_2^{-/-}$ mice were treated with CCl_4 for 4 weeks. Representative liver histology with Masson's trichrome staining of wild-type and $SIP_2^{-/-}$ mice is shown (A). Bar = 100 μ m. Arrows indicate the formation of fibrotic septa. The extent of liver fibrosis in CCl_4 - and olive oil (vehicle)-treated wild-type and $SIP_2^{-/-}$ mice was quantitated by calculating the ratio of the area of fibrosis to the area of section using Scion Image (B). Columns and bars represent means \pm SEM of five animals. The asterisk indicates a significant difference between CCl_4 -treated wild-type and $SIP_2^{-/-}$ mice in ANOVA followed by Tukey's honestly significant differences (Tukey's HSD) ($P < 0.05$).

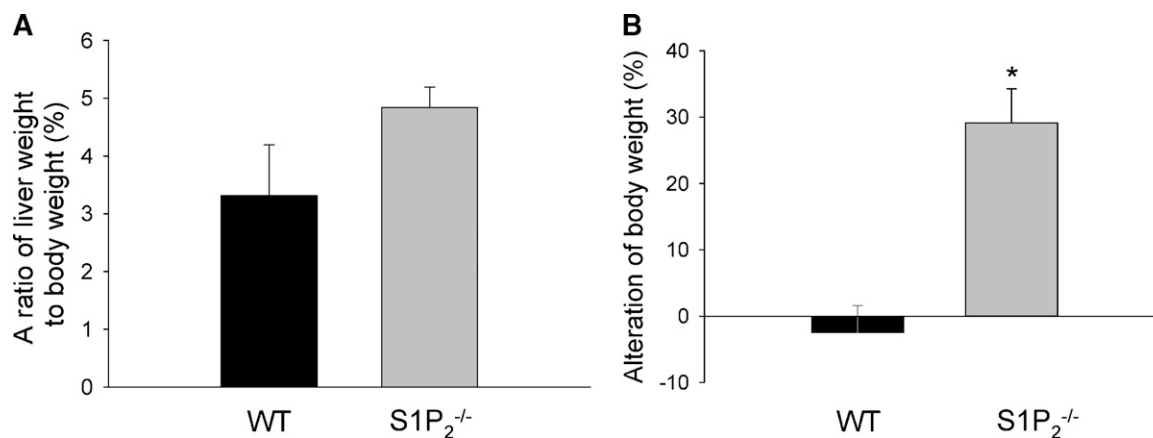


Fig. 6. The ratio of liver weight to body weight and body weight loss in wild-type and SIP₂^{-/-} mice after chronic CCl₄ administration. CCl₄ injection was performed for 4 weeks in wild-type (WT) and SIP₂^{-/-} mice. The ratio of liver weight to body weight was measured at euthanization after CCl₄ treatment (A). The alteration of body weight was determined by comparison of body weight at the first administration of CCl₄ and at euthanization after the last administration of CCl₄ (B). Columns and bars represent means \pm SEM of five animals. The asterisk indicates a significant difference from wild type in Student's *t*-test ($P < 0.05$).

with bridging fibrosis in the liver, whereas in SIP₂^{-/-} mice, such dense fibrotic septum development with nodule formation was not found (Fig. 5A). Quantitative analysis of fibrosis development revealed that the mean fibrotic area in the livers in wild-type mice was significantly larger than that in SIP₂^{-/-} mice treated with CCl₄. The extent of liver fibrosis in SIP₂^{-/-} mice was approximately 40% that of wild-type mice (Fig. 5B). On the other hand, liver histology in SIP₂^{-/-} mice administered olive oil alone, i.e., without CCl₄ treatment, was essentially unaltered compared with that of wild-type mice administered identically (Fig. 5B). In addition, serum ALT levels at the time of euthanization after chronic CCl₄ administration for 4 weeks were essentially unaltered in wild-type and SIP₂^{-/-} mice; 58 ± 20 IU/l ($n = 5$) and 51 ± 30 IU/l ($n = 5$), respectively. These results suggest that SIP₂ inactivation causes less liver fibrosis in response to chronic CCl₄ administration.

We examined the ratio of liver weight to body weight at euthanization after chronic CCl₄ administration. The trend of higher ratio of liver weight to body weight in SIP₂^{-/-} mice than in wild-type mice was noted ($P = 0.1475$) (Fig. 6A); 3.3% in wild-type and 4.8% in SIP₂^{-/-} mice. On the other hand, in mice treated with olive oil alone, the ratio of liver weight to body weight was not different with or without SIP₂ inactivation (data not shown). Alterations of body weight in wild-type and SIP₂^{-/-} mice with chronic CCl₄ administration were then examined by analysis of body weights at the first administration of CCl₄ and at euthanization after chronic CCl₄ administration. Repeated CCl₄ administration for 4 weeks caused no increase in body weight in wild-type mice, but a 25.6% increase in SIP₂^{-/-} mice (Fig. 6B). This body weight gain in SIP₂^{-/-} mice after chronic CCl₄ administration was comparable to that in both wild-type and SIP₂^{-/-} mice treated with olive oil alone for 4 weeks. Accordingly, only wild-type mice treated with CCl₄ for 4 weeks had much less weight gain. These data may be compatible with the finding that CCl₄-induced liver fibrosis was abrogated in SIP₂^{-/-} mice.

Both hepatic stellate cells and hepatic myofibroblasts are thought to be the principal matrix-producing cells with smooth-muscle α -actin expression, although controversy still exists as to whether hepatic myofibroblasts are distinct from hepatic stellate cells (28, 39). Thus, smooth-muscle α -actin expression in the liver is considered to be a marker of

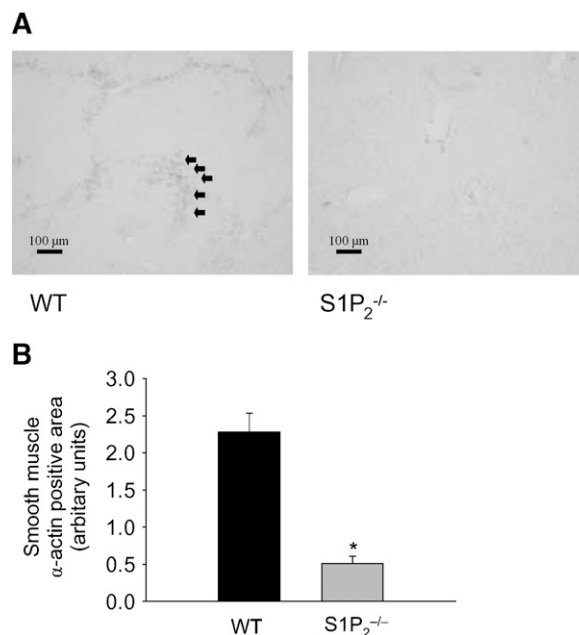


Fig. 7. Smooth-muscle α -actin-positive cells in wild-type and SIP₂^{-/-} livers after chronic CCl₄ administration. Immunohistochemical staining for smooth-muscle α -actin was performed in liver tissue as described in Materials and Methods, and representative results are shown in wild-type (WT) and SIP₂^{-/-} mice after chronic CCl₄ administration (A). Bar = 100 μ m. The extent of accumulation of smooth-muscle α -actin-positive cells (arrows) was quantitated using Scion Image (B). Columns and bars represent means \pm SEM of five animals. The asterisk indicates a significant difference from wild type in ANOVA followed by Tukey's HSD ($P < 0.05$).

the matrix-producing cells in the liver. Chronic CCl₄ administration caused a significant accumulation of smooth-muscle α -actin-positive cells in wild-type livers, whereas it was less apparent in SIP₂^{-/-} livers (Fig. 7A). Quantitative analysis revealed that the smooth-muscle α -actin-positive cell area was reduced by 78% in SIP₂^{-/-} livers compared with wild-type livers (Fig. 7B). Thus, these results suggest that SIP₂ inactivation leads to decreased accumulation of the matrix-producing cells in the liver, namely hepatic stellate cells and/or hepatic myofibroblasts, in CCl₄-induced liver fibrosis.

DISCUSSION

In the current study, liver regeneration was enhanced in SIP₂^{-/-} mice compared with wild-type mice after acute liver injury induced by a single injection of CCl₄ or DMN, suggesting that SIP may be involved in liver regeneration, possibly as an inhibitory regulator via SIP₂. This was determined by the increased nuclear labeling with BrdU and immunohistochemical staining of PCNA in hepatocytes and by the enhanced ratio of liver weight to body weight in SIP₂^{-/-} mice compared with wild-type mice in CCl₄-induced acute liver injury. On the other hand, in DMN-induced acute liver injury, increased liver regeneration was determined by the increased immunohistochemical staining of PCNA in hepatocytes in SIP₂^{-/-} mice compared with wild-type mice, although the enhanced ratio of liver weight to body weight was not found in SIP₂^{-/-} mice. Because submassive hemorrhagic necrosis is characteristic of DMN-intoxicated liver (36), the resultant congestion in the liver may affect the exact weight determination of liver parenchyma. Furthermore, higher survival rate after DMN intoxication with a lethal dose (35) in SIP₂^{-/-} mice compared with wild-type mice was determined. This may be explained by increased liver regeneration, and the SIP₂ antagonist merits consideration as a therapeutic agent for liver failure caused by impaired liver regeneration. Because the liver damage evaluated by liver function tests was not different between wild-type and SIP₂^{-/-} mice in both CCl₄- and DMN-induced liver injury, the enhanced liver regeneration in SIP₂^{-/-} mice may not be due to a response to the enhanced liver damage. Collectively, the current evidence has suggested that SIP plays a physiological role in liver regeneration via SIP₂ as a negative regulator.


A recent study by Serrier-Lanneau et al. (23) reported that the regenerative response after a single injection of CCl₄ in SIP₂^{-/-} mice was not different from that in wild-type mice, where liver regeneration was assessed by Western blot analysis of PCNA expression in the liver. In our study, immunohistochemical analysis of PCNA revealed that PCNA-positive hepatocytes were increased in SIP₂^{-/-} livers by 1.7-fold compared with wild-type livers at 48 h after CCl₄ administration. Another interesting finding was that PCNA-positive nonparenchymal cells were found in significant numbers in wild-type livers, but were much less apparent in SIP₂^{-/-} livers, which may be in line with the finding by Serrier-Lanneau et al. (23) that hepatic myofibroblasts

from SIP₂^{-/-} livers were less regenerative compared with those from wild-type livers after a single CCl₄ injection. It is likely that Western blot analysis of PCNA expression in the whole-liver extracts determined regeneration in both nonparenchymal cells and hepatocytes. We would also assume that a less than 2-fold increase may occasionally be difficult to detect by Western blot analysis, inasmuch as our Western blot analysis did not reveal significant differences in PCNA expression between wild-type and SIP₂^{-/-} livers (data not shown).

On the other hand, liver fibrosis induced by chronic CCl₄ administration was less apparent in SIP₂^{-/-} mice than in wild-type mice. The reduced body weight loss in SIP₂^{-/-} mice after chronic CCl₄ administration may be compatible with the reduction of CCl₄-induced liver fibrosis in SIP₂^{-/-} mice. Such evidence indicates that SIP₂ inactivation leads to reduced liver fibrosis induced by CCl₄, suggesting that SIP and SIP₂ may play a role in the development of liver fibrosis.

The reduction of liver fibrosis in SIP₂ inactivation may not be explained by the alteration in the extent of liver damage by CCl₄, because the liver damage was essentially the same in wild-type and SIP₂^{-/-} mice. Instead, the reduced accumulation of smooth-muscle α -actin-positive cells in the livers of SIP₂^{-/-} mice treated with CCl₄ for 4 weeks may be a key to the reduced liver fibrosis in those mice, because smooth-muscle α -actin-positive cells in the liver are assumed to be the principal matrix-producing cells of the diseased liver, namely hepatic stellate cells and hepatic myofibroblasts (29).

We previously showed abundant mRNA expression of SIP₁ and SIP₂ in both hepatocytes (18) and hepatic stellate cells (16) in rats. On the other hand, increased mRNA expression of SIP₂ and SIP₃ and unaltered mRNA expression of SIP₁ in the liver after a single CCl₄ injection were reported in mice (23). Although our current evidence suggests that SIP₂ may play a significant role in the response to liver injury, the significance of abundant expression of SIP₁ in liver cells and upregulation of SIP₃ expression in the liver after injury remains to be examined.

Recent evidence suggests that SIP receptors regulate important physiological functions of the vascular system, such as vascular morphogenesis and maturation, cardiac function, vascular permeability, and tumor angiogenesis (40–43). Our current evidence suggests that SIP₂ may also play a significant role in liver pathophysiology. 

REFERENCES

1. Spiegel, S., and A. H. Merrill, Jr. 1996. Sphingolipid metabolism and cell growth regulation. *FASEB J.* **10**: 1388–1397.
2. Olivera, A., and S. Spiegel. 1993. Sphingosine-1-phosphate as second messenger in cell proliferation induced by PDGF and FCS mitogens. *Nature*. **365**: 557–560.
3. Rani, C. S., F. Wang, E. Fuior, A. Berger, J. Wu, T. W. Sturgill, D. Beitner-Johnson, D. LeRoith, L. Varticovski, and S. Spiegel. 1997. Divergence in signal transduction pathways of platelet-derived growth factor (PDGF) and epidermal growth factor (EGF) receptors. Involvement of sphingosine 1-phosphate in PDGF but not EGF signaling. *J. Biol. Chem.* **272**: 10777–10783.

4. Cuvillier, O., G. Pirianov, B. Kleuser, P. G. Vanek, O. A. Coso, S. Gutkind, and S. Spiegel. 1996. Suppression of ceramide-mediated programmed cell death by sphingosine-1-phosphate. *Nature*. **381**: 800–803.
5. Edsall, L. C., G. G. Pirianov, and S. Spiegel. 1997. Involvement of sphingosine 1-phosphate in nerve growth factor-mediated neuronal survival and differentiation. *J. Neurosci.* **17**: 6952–6960.
6. Goodemote, K. A., M. E. Mattie, A. Berger, and S. Spiegel. 1995. Involvement of a pertussis toxin-sensitive G protein in the mitogenic signaling pathways of sphingosine 1-phosphate. *J. Biol. Chem.* **270**: 10272–10277.
7. Tosaka, M., F. Okajima, Y. Hashiba, N. Saito, T. Nagano, T. Watanabe, T. Kimura, and T. Sasaki. 2001. Sphingosine 1-phosphate contracts canine basilar arteries in vitro and in vivo: possible role in pathogenesis of cerebral vasospasm. *Stroke*. **32**: 2913–2919.
8. Ohmori, T., Y. Yatomi, M. Osada, F. Kazama, T. Takafuta, H. Ikeda, and Y. Ozaki. 2003. Sphingosine 1-phosphate induces contraction of coronary artery smooth muscle cells via S1P2. *Cardiovasc. Res.* **58**: 170–177.
9. Ishii, I., N. Fukushima, X. Ye, and J. Chun. 2004. Lysophospholipid receptors: signaling and biology. *Annu. Rev. Biochem.* **73**: 321–354.
10. Gardell, S. E., A. E. Dubin, and J. Chun. 2006. Emerging medicinal roles for lysophospholipid signaling. *Trends Mol. Med.* **12**: 65–75.
11. Yatomi, Y., F. Ruan, J. Ohta, R. J. Welch, S. Hakomori, and Y. Igarashi. 1995. Quantitative measurement of sphingosine 1-phosphate in biological samples by acylation with radioactive acetic anhydride. *Anal. Biochem.* **230**: 315–320.
12. Pappu, R., S. R. Schwab, I. Cornelissen, J. P. Pereira, J. B. Regard, Y. Xu, E. Camerer, Y. W. Zheng, Y. Huang, J. G. Cyster, et al. 2007. Promotion of lymphocyte egress into blood and lymph by distinct sources of sphingosine-1-phosphate. *Science*. **316**: 295–298.
13. Chun, J. 2007. Immunology. The sources of a lipid conundrum. *Science*. **316**: 208–210.
14. Yang, A. H., I. Ishii, and J. Chun. 2002. In vivo roles of lysophospholipid receptors revealed by gene targeting studies in mice. *Biochim. Biophys. Acta.* **1582**: 197–203.
15. Herr, D. R., N. Grillet, M. Schwander, R. Rivera, U. Muller, and J. Chun. 2007. Sphingosine 1-phosphate (S1P) signaling is required for maintenance of hair cells mainly via activation of S1P2. *J. Neurosci.* **27**: 1474–1478.
16. Ikeda, H., Y. Yatomi, M. Yanase, H. Satoh, H. Maekawa, I. Ogata, Y. Ozaki, Y. Takuwa, S. Mochida, and K. Fujiwara. 2000. Biological activities of novel lipid mediator sphingosine 1-phosphate in rat hepatic stellate cells. *Am. J. Physiol. Gastrointest. Liver Physiol.* **279**: G304–G310.
17. Ikeda, H., K. Nagashima, M. Yanase, T. Tomiya, M. Arai, Y. Inoue, K. Tejima, T. Nishikawa, N. Watanabe, M. Omata, et al. 2004. Sphingosine 1-phosphate enhances portal pressure in isolated perfused liver via S1P2 with Rho activation. *Biochem. Biophys. Res. Commun.* **320**: 754–759.
18. Ikeda, H., H. Satoh, M. Yanase, Y. Inoue, T. Tomiya, M. Arai, K. Tejima, K. Nagashima, H. Maekawa, N. Yahagi, et al. 2003. Antiproliferative property of sphingosine 1-phosphate in rat hepatocytes involves activation of Rho via Edg-5. *Gastroenterology*. **124**: 459–469.
19. Michalopoulos, G. K., and M. C. DeFrances. 1997. Liver regeneration. *Science*. **276**: 60–66.
20. Friedman, S. L. 2000. Molecular regulation of hepatic fibrosis, an integrated cellular response to tissue injury. *J. Biol. Chem.* **275**: 2247–2250.
21. Minato, Y., Y. Hasumura, and J. Takeuchi. 1983. The role of fat-storing cells in Disse space fibrogenesis in alcoholic liver disease. *Hepatology*. **3**: 559–566.
22. Rockey, D. C., C. N. Housset, and S. L. Friedman. 1993. Activation-dependent contractility of rat hepatic lipocytes in culture and in vivo. *J. Clin. Invest.* **92**: 1795–1804.
23. Serriere-Lanneau, V., F. Teixeira-Clerc, L. Li, M. Schippers, W. de Wries, B. Julien, J. Tran-Van-Nhieu, S. Manin, K. Poelstra, J. Chun, et al. 2007. The sphingosine 1-phosphate receptor S1P2 triggers hepatic wound healing. *FASEB J.* **21**: 2005–2013.
24. Adachi, M., Y. Osawa, H. Uchinami, T. Kitamura, D. Accili, and D. A. Brenner. 2007. The forkhead transcription factor FoxO1 regulates proliferation and transdifferentiation of hepatic stellate cells. *Gastroenterology*. **132**: 1434–1446.
25. Kojima, N., M. Hori, T. Murata, Y. Morizane, and H. Ozaki. 2007. Different profiles of Ca²⁺ responses to endothelin-1 and PDGF in liver myofibroblasts during the process of cell differentiation. *Br. J. Pharmacol.* **151**: 816–827.
26. Park, E. J., Y. Z. Zhao, Y. C. Kim, and D. H. Sohn. 2007. Bakuchiol-induced caspase-3-dependent apoptosis occurs through c-Jun NH2-terminal kinase-mediated mitochondrial translocation of Bax in rat liver myofibroblasts. *Eur. J. Pharmacol.* **559**: 115–123.
27. Watson, M. R., K. Wallace, R. G. Gieling, D. M. Manas, E. Jaffray, R. T. Hay, D. A. Mann, and F. Oakley. 2008. NF-kappaB is a critical regulator of the survival of rodent and human hepatic myofibroblasts. *J. Hepatol.* **48**: 589–597.
28. Knittel, T., D. Kobold, B. Saile, A. Grundmann, K. Neubauer, F. Piscaglia, and G. Ramadori. 1999. Rat liver myofibroblasts and hepatic stellate cells: different cell populations of the fibroblast lineage with fibrogenic potential. *Gastroenterology*. **117**: 1205–1221.
29. Saile, B., N. Matthes, K. Neubauer, C. Eisenbach, H. El-Armouche, J. Dudas, and G. Ramadori. 2002. Rat liver myofibroblasts and hepatic stellate cells differ in CD95-mediated apoptosis and response to TNF-alpha. *Am. J. Physiol. Gastrointest. Liver Physiol.* **283**: G435–G444.
30. Ishii, I., X. Ye, B. Friedman, S. Kawamura, J. J. Contos, M. A. Kingsbury, A. H. Yang, G. Zhang, J. H. Brown, and J. Chun. 2002. Marked perinatal lethality and cellular signaling deficits in mice null for the two sphingosine 1-phosphate (S1P) receptors, S1P(2)/LP(B2)/EDG-5 and S1P(3)/LP(B3)/EDG-3. *J. Biol. Chem.* **277**: 25152–25159.
31. Goparaju, S. K., P. S. Jolly, K. R. Watterson, M. Bektas, S. Alvarez, S. Sarkar, L. Mel, I. Ishii, J. Chun, S. Milstien, et al. 2005. The S1P2 receptor negatively regulates platelet-derived growth factor-induced motility and proliferation. *Mol. Cell. Biol.* **25**: 4237–4249.
32. Means, C. K., C. Y. Xiao, Z. Li, T. Zhang, J. H. Omens, I. Ishii, J. Chun, and J. H. Brown. 2007. Sphingosine 1-phosphate S1P2 and S1P3 receptor-mediated Akt activation protects against in vivo myocardial ischemia-reperfusion injury. *Am. J. Physiol. Heart Circ. Physiol.* **292**: H2944–H2951.
33. Simeonova, P. P., R. M. Gallucci, T. Hulderman, R. Wilson, C. Kommineni, M. Rao, and M. I. Luster. 2001. The role of tumor necrosis factor-alpha in liver toxicity, inflammation, and fibrosis induced by carbon tetrachloride. *Toxicol. Appl. Pharmacol.* **177**: 112–120.
34. Kanno, K., S. Tazuma, and K. Chayama. 2003. AT1A-deficient mice show less severe progression of liver fibrosis induced by CCl(4). *Biochem. Biophys. Res. Commun.* **308**: 177–183.
35. Morrison, V., and J. Ashby. 1994. Reconciliation of five negative and four positive reports of the activity of dimethylnitrosamine in the mouse bone marrow micronucleus assay. *Mutagenesis*. **9**: 361–365.
36. Jin, Y. L., H. Enzan, N. Kuroda, Y. Hayashi, H. Nakayama, Y. H. Zhang, M. Toi, E. Miyazaki, M. Hiroi, L. M. Guo, et al. 2003. Tissue remodeling following submassive hemorrhagic necrosis in rat livers induced by an intraperitoneal injection of dimethylnitrosamine. *Virchows Arch.* **442**: 39–47.
37. Bedossa, P., and T. Poynard. 1996. An algorithm for the grading of activity in chronic hepatitis C. The METAVIR Cooperative Study Group. *Hepatology*. **24**: 289–293.
38. Caballero, T., A. Perez-Milena, M. Maseroli, F. O'Valle, F. J. Salmeron, R. M. Del Moral, and G. Sanchez-Salgado. 2001. Liver fibrosis assessment with semiquantitative indexes and image analysis quantification in sustained-responder and non-responder interferon-treated patients with chronic hepatitis C. *J. Hepatol.* **34**: 740–747.
39. Rockey, D. C., J. K. Boyles, G. Gabbiani, and S. L. Friedman. 1992. Rat hepatic lipocytes express smooth muscle actin upon activation in vivo and in culture. *J. Submicrosc. Cytol. Pathol.* **24**: 193–203.
40. Sanchez, T., T. Estrada-Hernandez, J. H. Paik, M. T. Wu, K. Venkataraman, V. Brinkmann, K. Claffey, and T. Hla. 2003. Phosphorylation and action of the immunomodulator FTY720 inhibits vascular endothelial cell growth factor-induced vascular permeability. *J. Biol. Chem.* **278**: 47281–47290.
41. Chae, S. S., J. H. Paik, H. Furneaux, and T. Hla. 2004. Requirement for sphingosine 1-phosphate receptor-1 in tumor angiogenesis demonstrated by in vivo RNA interference. *J. Clin. Invest.* **114**: 1082–1089.
42. LaMontagne, K., A. Littlewood-Evans, C. Schnell, T. O'Reilly, L. Wyder, T. Sanchez, B. Probst, J. Butler, A. Wood, G. Liao, et al. 2006. Antagonism of sphingosine-1-phosphate receptors by FTY720 inhibits angiogenesis and tumor vascularization. *Cancer Res.* **66**: 221–231.
43. Sanna, M. G., S. K. Wang, P. J. Gonzalez-Cabrera, A. Don, D. Marsolais, M. P. Matheu, S. H. Wei, I. Parker, E. Jo, W. C. Cheng, et al. 2006. Enhancement of capillary leakage and restoration of lymphocyte egress by a chiral S1P1 antagonist in vivo. *Nat. Chem. Biol.* **2**: 434–441.